https://doi.org/10.5194/hess-2024-214
Preprint. Discussion started: 9 September 2024

Hydrology and Earth System Sciences
Open Access
Discussions

Reinforce lake water balance components estimations by integrating water isotope compositions with a hydrological model

Nariman Mahmoodi[1, 2*], Ulrich Struck[3], Michael Schneider[1] Christoph Merz[1, 2]

[1] Department of Hydrogeology, Institute of Geological Sciences, Freie Universität Berlin, Berlin, Germany

[2] Lowland Hydrology and Water Management Group, Leibniz Centre for Agricultural Landscape Research (ZALF), Müncheberg, Germany

[3] Museum für Naturkunde, Leibniz-Institut für Evolutions- und Biodiversitätsforschung, Berlin, Germany

[*]Corresponding author, email: n.mahmoodi@fu-berlin.de

Abstract:

Accurate estimation of water balance components of groundwater-fed lakes, including subsurface inflow, as well as actual evaporation from lakes, poses a complex task for hydrologists employing hydrological models. Hence, an alternative approach was used to capture the dynamic behavior of the hydrological groundwater/surface water system, which can be used for integration with the hydrological model and serves as a validation for the hydrological model estimates of the water balance components. The approach, based on measurements of the stable isotopes ($\delta^{18}O$ and δD) enables the quantitative estimation of the individual water flux and evapotranspiration rates. An isotope-mass-balance model was used to quantify lake water balances over a one-year sampling period. The approach is based on the global relationship between the $\delta^{18}O$ and δD values of the precipitation and kinetic isotopic fractionation in the lake water during evaporation. Assuming that the lake is hydrostatically connected to the groundwater the isotope mass-balance model accounts for the quantification of the evapotranspiration rate considering the groundwater inflow compensating the evaporation loss. The study addresses the model-based quantification of subsurface-groundwater inflow and evaporation losses of a young glacial groundwater lake (Lake Gross Glienicke (GG), southwest of Berlin in the Havel catchment), over the period from 2015 to 2023 with the integrated hydrological model HydroGeoSphere. Utilizing the isotopic mass balance model, HydroCalculator, under steady-state hydrologic regime conditions, the evaporation-to-inflow (E/I) ratio is determined for the period of one year spanning August 2022 to September 2023. Employing the fully integrated hydrological model, calibrated and validated under monthly normal transient flow conditions from 2008 to 2023 for the lake

https://doi.org/10.5194/hess-2024-214
Preprint. Discussion started: 9 September 2024

Hydrology and Earth System Sciences
Open Access
Discussions

catchment, subsurface, and groundwater inflows to the lake are calculated and compared to the calculated E/I ratios based on the isotopic measurement of the lake water. Isotopic signatures of surface water, groundwater, and rainwater ($\delta^{18}O$ and δD) confirm a flow-through type for the lake. The calculated E/I ratio for GG Lake is around 40%. The calculated evaporation for the years 2022 and 2023, within the isotopic mass balance model framework (E_{iso22} = 601 mm, E_{iso23} = 553 mm), aligns well with the actual evaporation from the lakes calculated by the HGS model (E_{HGS22} = 688 mm, E_{HGS23} = 659 mm). The change in the ratio of evaporation to inflow (E/I) leads to a significantly improved estimation of evaporation rates after correction for temperature fluctuations and inflow data from previous years (2015-2021). With a correlation coefficient of 0.81, these revised estimates show a high degree of agreement with the evaporation rates predicted by the HydroGeoSphere (HGS) model for the corresponding years. Despite the uncertainties associated with the analysis of the water isotope signature, its integration into the hydrological model serves to validate the hydrological model calculations of the water balance components.

Keywords: HydroGeoSphere, HydroCalculator, Lake Water Exchange, Evaporation Loses, Stable Isotope, Gross Glienicke Lake

1. Introduction

Hydrological models have undergone substantial advancements in past decades (Singh, 2018; Herrera et al., 2022), but still face unsolved problems and uncertainties in depicting hydrological processes (Liu and Gupta, 2007; Renard et al., 2010). Recently, a wide range of monitoring and modeling techniques have emerged for investigating water fluxes at different scales (Fekete et al., 2006, Windhorst et al., 2014). However, limitations in the hydrological model parametrizations lead to insufficient quantification of water flows, and therefore a quantitatively and qualitatively incorrect interpretation of hydrodynamic processes and, as a result, inaccurate assumptions for water management purposes (Müller Schmied et al., 2014). Improving the informative value of the models, representing complex hydrological processes is needed to enhance the applicability of the models for future estimations and scenario analyses. The optimal adaptation of hydrological models to real conditions for a precise determination of water balance components is often considered unattainable within the current technical possibilities due to the overwhelming amount of work associated with field measurements. Particularly the quantification of groundwater-surface water exchange using

https://doi.org/10.5194/hess-2024-214
Preprint. Discussion started: 9 September 2024

the hydrological models faces pronounced uncertainties in considering geostructural heterogeneities in different scales. To validate the model results, arduous monitoring surveys are required to measure for example the groundwater-surface water interactions along rivers' banks or lakes' shorelines (Partington, 2020). Hence, a combination of hydrogeological modeling, field measurements, and innovative isotopic-based studies along with appropriate linkage between these approaches will be a concrete way to achieve optimal parameterization and validation capabilities for modeling hydrological processes in complex geohydraulic systems.

Recent studies show that the stable water isotope mass balance on different water sources together with the numerical models improve the model performance in simulating the interactions between groundwater and surface water (e.g., Jafari et al., 2021). The isotopic insights enhance hydrogeologists' efforts to calculate water balance components such as the groundwater inflow to the surface water resources and water losses due to evaporation (Skrzypek et al., 2015; Vyse et al., 2020). This method is based on the fractionation of heavier isotopes caused by evaporation from surface water, provoking a disparity in isotopic composition between groundwater and surface water. However, a limitation of this approach is that the stable water isotope mass balance is restricted to the sampling time, making it incapable of accounting for the transient behavior of groundwater-surface water exchange over different time periods. Although water isotope tests can describe the changes in water fluxes in specific time frame intervals (e.g. monthly), deficiency in providing spatial exchanges between groundwater and surface water can be also introduced as their limitation. These gaps can be addressed by integrating water isotope analyses with physical-based hydrogeological models.

Water isotope analyses are helpful techniques to evaluate the model's performance. For instance, Ala-Aho et al. (2015) assess the hydrogeological model performance by comparing the simulated groundwater inflow to lakes in the middle of Finland with calculated recharge by water isotope analyses.

In the northeast of Germany, groundwater levels and landscape runoff have largely been in decline for over three decades (Lahmer 2003; Germer et al., 2011; Merz and Pekdeger, 2011); regional climate studies suggest further decreases over the next decades (Gerstengarbe et al., 2003, 2013). Thus, water resource management for this region requires a thorough assessment of possible adaptions and measures to counteract or mitigate severe consequences, such as decreasing groundwater heads and surface water levels and declining groundwater and surface

https://doi.org/10.5194/hess-2024-214
Preprint. Discussion started: 9 September 2024

Hydrology and Earth System Sciences
Discussions

water quality. The development of integrated management schemes for groundwater-dependent ecosystems such as lakes under climate changes, requires a more comprehensive understanding of hydrological dynamics and a better estimation of ecologically relevant water fluxes are of prime importance. Therefore, an alternative approach was developed to capture the complex behavior of the hydrological groundwater-surface water system. This approach can be integrated with hydrological models to improve parameterization and validate model calculations in water balance components.

2. Materials and methods

2.1 Study area

Gross Glienicke Lake (GGS) with an area of 0.59 km^2 and a maximum depth of 10 meters is located in Berlin-Brandenburg state, Germany (30–87 m.s.l., Fig. 1a). It is a young glacial lowland lake that is exclusively fed by groundwater. The lake's water levels have shown significant seasonal variability (around 0.4 m) over recent decades (Fig. 2). Since 2014 the lake’s water level has faced severe drops (Fig. 2) around 1.28 meters. GGS as a seepage lake (lake without an outlet) is surrounded by low-density residences (Fig. 1). In the north and northwestern areas, grassland and farmland are the dominant surface cover and directly overly sandy soils. The aquifers are recharged in the Döberitzer-Heide region where fine sandy soil with a hydraulic conductivity ranging from 8 × 10^{-5} to 12× 10^{-5} m/s can be found according to the lab analysis. The root zone within the grassland ranges in depth from the surface to 30 cm. The groundwater monitoring measurements illustrate a smooth hydraulic head gradient from West to East, highlighting connections between the lake and the aquifer recharge area from the Döberitzer-Heide region (Fig. 3). On the east side of the lake catchment, a regulated river, the Havel, has been flowing from northeast to southwest. Continuous stratigraphic units have been delineated throughout the lakes’ catchment based on the geological features information collected from 480 boreholes (Fig. 2, The Federal Institute for Geosciences and Natural Resources - BGR 2022). The geology in the study area is formed by a series of layered Pleistocene and Tertiary sediments that are approximately 150 to 200 m thick, with a lower confining bed of Oligocene marine Rupel clay. The series consists of a complex interplay of glacial deposits from the Pleistocene and permeable marine and limnic sediments of the Upper Oligocene and Miocene. The series can be divided into an upper unconfined aquifer system of shallow Weichselian and late Saalian sediments. In general, a shallow (i.e., 5 to 10

https://doi.org/10.5194/hess-2024-214
Preprint. Discussion started: 9 September 2024

m) unconfined aquifer is separated from the thick (140 to 190 m) lower confined aquifer by a 15 to 20 m thick layer of Saalian sediments. The confined and unconfined aquifers consist of multiple permeable sediment layers partially disconnected by layers of till, but still hydraulically connected. The hydraulic connection to the lakes is mainly controlled by these aquifer layers. Underneath these sediments is a thick confined aquifer system of the early Saalian and Elster layers, and Upper Oligocene and Miocene sediments. The first shallow, unconfined aquifer in the catchment area is characterized by highly permeable glacial sand and gravel deposits (Holocene and Weichselian). A till layer (Weichselian age, Fig. 3) is found in the underlying layers. The till is underlain by late Warthe sandy sediments forming the second aquifer.

2.2 Available meteorological data

From 1990 to 2023, radar-based CER v2 data (The Central Europe Refined Analysis version 2, details on the data pre- and past-processing are provided by Jänicke et al., 2017) generated a mean daily temperature of 10.4 °C and average annual precipitation of 612 mm, with an average annual actual evapotranspiration (PET) of 639, 646, and 670 mm for farmland and grassland, forest, and urban areas respectively. The annual mean humidity in Gatow station varies from 50% to 70% over the last two decades (2000-2023). During the hydrological year of the survey (August 2022 to September 2023), the mean precipitation, temperature, and humidity in the study region were 51.9 mm, 12.3 ˚C (Potsdam weather station, DWD, 2024;), and 69 % respectively (recorded in Gatow weather station of The Berlin Measurement Network (MEVIS, Fig. 1). Precipitation data as one of the boundary conditions in the modeling work has been obtained from the Potsdam station of the German Weather Service (DWD, 2024).

https://doi.org/10.5194/hess-2024-214
Preprint. Discussion started: 9 September 2024

Hydrology and Earth System Sciences Discussions

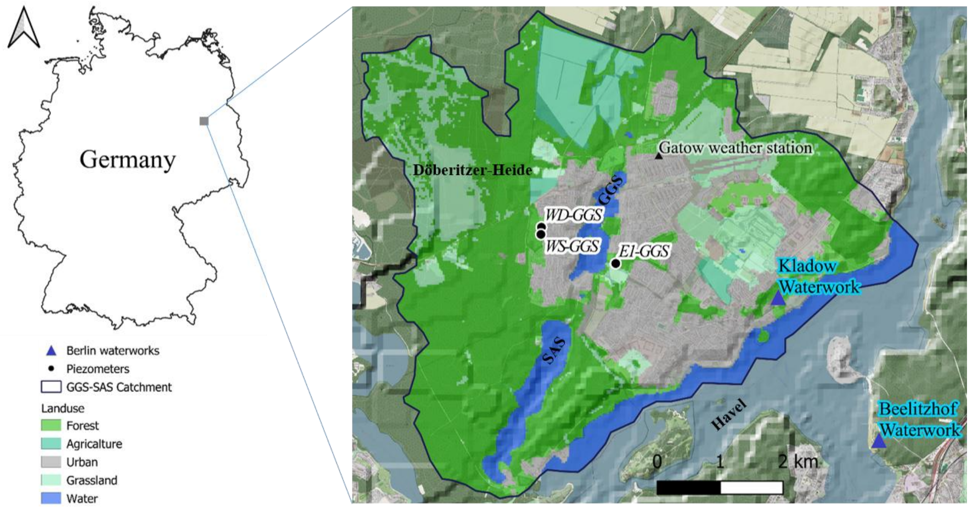

Fig. 1. Location of the study area, highlighting Gross Glienicke Lake (GGS), Sacrow Lake (SAS), Havel channel, piezometers on the east (E-GGS) and west (WD-GGS and WS-GGS) side of GGS, Berlin waterworks, and land use classifications. © OpenStreetMap contributors 2023. Distributed under the Open Data Commons Open Database License (ODbL) v1.0..

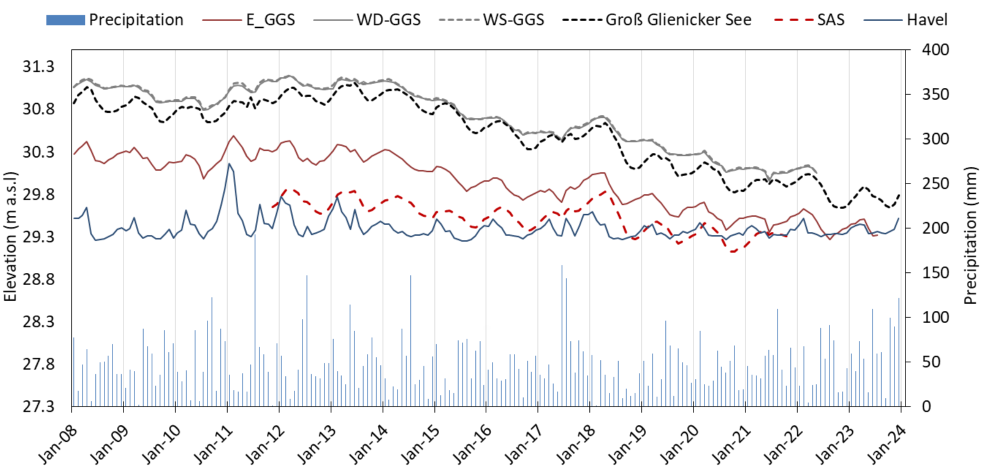

Fig. 2. Lakes water level fluctuations and precipitation variations during the period of 2008 to 2023.

https://doi.org/10.5194/hess-2024-214
Preprint. Discussion started: 9 September 2024

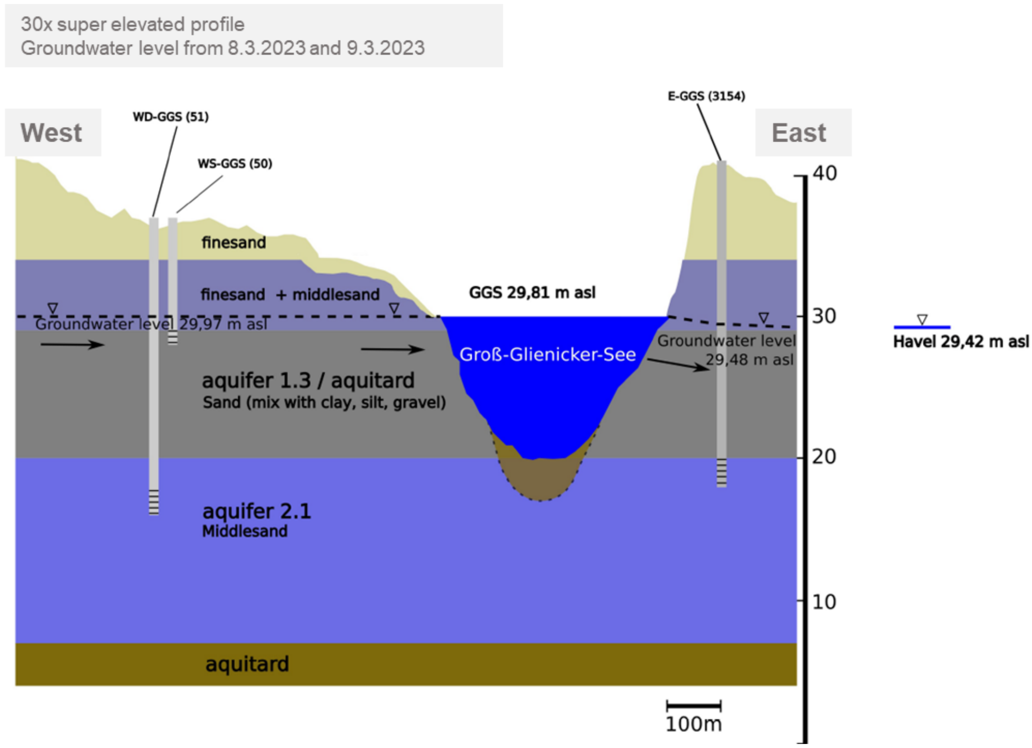

Fig. 3. Conceptual cross-section of the aquifer demonstrating the geological structure, the hydraulic head, and water flow direction from the groundwater recharge area towards Gross Glienicke Lake (GGS) and the groundwater discharge area with a lower altitude. WD-GGS, WS-GGS, and E-GGS are the piezometers on the west and east sides of GGS.

2.2 Stable isotope analysis

Surface water samples were collected for one year (from August 2022 to September 2023) on a monthly time interval from GGS and three piezometers installed in the first two aquifers, encompassing the lakes, and from two rainwater samplers. The total depth and well water volume of the monitoring well, and the stability of in-situ parameters such as temperature, pH, and electrical conductivity (EC) were monitored as guidance of appropriate timing for water sampling from the piezometers. All water samples collected in clusters within two-day excursions were filtered through a membrane filter (0.2 and 0.45-µm pore) and stored at 6 °C to prevent evaporation before laboratory analysis. Stable isotope ratios of oxygen ($^{18}O/^{16}O$) and hydrogen ($^{2}H/^{1}H$) in H^2O in water samples were measured with a PICARRO L1102-i isotope analyzer. The L1102-i is based on the WS-CRDS (wavelength-scanned cavity ring-

https://doi.org/10.5194/hess-2024-214
Preprint. Discussion started: 9 September 2024

Hydrology and Earth System Sciences Discussions
Open Access EGU

down spectroscopy) technique (Gupta et al., 2009). Measurements were calibrated by the application of linear regression of the analyses of IAEA calibration material VSMOW, VSLAP, and GISP. The stable isotope ratios of oxygen and hydrogen are expressed in the conventional delta notation ($\delta^{18}O$, δD) per mil (‰) versus VSMOW. For each sample 6 replicate injections were performed and arithmetic average and standard deviations (1 sigma) were calculated. The reproducibility of replicate measurements is generally better than 0.1 ‰ for oxygen and 0.5 ‰ for hydrogen.

2.3 Isotope mass balance model

The evaporation loss from a lake such as GGS Lake can be calculated by knowing the transient stable water isotope compositions of inflow and moisture in ambient air and climate data (air temperature and humidity) for the specific period of time and considering a steady-state hydrologic condition (no additional water inflows, Tweed et al. 2009; Gibson and Reid, 2010). The isotope mass balance model (Hydrocalculator) whose capability has been verified through various field experiments globally (Skrzypek et al. 2015; Vyse et al., 2020) was applied to estimate evaporation over inflow ratio (E/I) for the GGS Lake in the steady state condition. The differences between stable isotope compositions of water samples reflect the isotopic phases: enrichment (heavier isotope) or dilution (lighter isotope). Hence, a series of time-based analyses enables the assessment of evaporation progress. Climate data from nearby weather stations (Gatow and Potsdam) were utilized to address uncertainties arising from the distance to the points of water samplings (Gibson and Reid, 2014; Skrzypek et al. 2015). The stable isotope composition of moisture in ambient air (δ_{air}) is estimated from the mean monthly weighted averages from the stable isotope composition of precipitation (δ_{pcp}) of GNIP station (GNIP/Berlin (DWD, BFG, BGR & HHZM, Stumpp et al. 2014 and Schmidt et al. 2020) which were corrected by local precipitation stable isotope composition. The δ_{air} is calculated based on the rain and rain-LEL as follows (Gibson and Reid, 2014):

$$\delta_{air} = (\delta_{pcp} - \varepsilon^{+})/(1+ \varepsilon^{+} \times 10^{-3}) \qquad \textbf{Eq. 1}$$

where ε^{+} is an isotope fractionation factor that is solely temperature-dependent. ε is the total fractionation factor, and equals the sum of the equilibrium isotope fractionation factor ε^{+}, as given above plus the kinetic isotope fractionation factor ε_k (Gibson and Reid, 2010):

$$\varepsilon = \varepsilon^{+} / (1+ \varepsilon^{+} \times 10^{-3}) + \varepsilon_k$$ **Eq. 2**

The kinetic fractionation ε_k is defined as (Gat 1995):

$$\varepsilon_k = (1- h) \times C_k$$ **Eq. 3**

According to Gonfiantini, 1986 and Araguas-Araguas et al., 2000, the kinetic fractionation constant (C_k) is 12.5 percent for δD and 14.2 percent for $\delta^{18}O$. Air relative humidity (h) is given as a fraction.

Based on the local climate conditions the enrichment of stable isotope compositions can be limited. According to Gat and Levy (1978) and Gat, (1981), this limitation threshold (δ^*) can be estimated by considering air humidity (h), $\delta_{air,}$ and a total enrichment factor (ε).

$$\delta^* = (h \times \delta_{air} + \varepsilon) / (h - \varepsilon \times 10^{-3})$$ **Eq. 4**

When this limitation exceeds, further evaporation does not result in isotope enrichment.

The ratio of evaporation over inflow (E/I) can be calculated using the following reformulated equation (e.g. as by Mayr et al. (2007)) under steady-state hydrological conditions. E/I is the fraction of inflowing water evaporated from GGS Lake:

$$E/I = ((\delta_{inflow} - \delta_{outflow}) / (\delta^* - \delta_{inflow}) \times E_s)$$ **Eq. 5**

enrichment slope (E_s) is defined by Welhan and Fritz, 1977 and Allison and Leaney, 1982 accordingly:

$$E_s = (h - (\varepsilon \times 10^{-3})) / (1 - h + (\varepsilon \times 10^{-3}))$$ **Eq. 6**

The model calculates the evaporative losses based on the theory behind the Craig–Gordon model (Gibson and Reid (2014)). The variables used in the Hydrocalculator model are listed in Table 1.

Table 1. The list of variables used in the Hydrocalculator model

Variable	Description	Unit
T	temperature	°C
h	air relative humidity	-

https://doi.org/10.5194/hess-2024-214
Preprint. Discussion started: 9 September 2024

Hydrology and Earth System Sciences
Discussions

δ_{air}	stable isotope composition of moisture in ambient air	%
δ_{pcp}	stable isotope composition of precipitation	%
LEL	slope of the local evaporation line	
ε	total isotope fractionation	%
ε^{+}	equilibrium isotope fractionation factor	%
ε_k	kinetic isotope fractionation factor	%
C_k	kinetic fractionation constant	
δ^{*}	limiting isotopic composition	%
E/I	Evaporation over inflow ratio	%
δ_{inflow}	stable isotope composition of inflow (groundwater)	%
$\delta_{outflow}$	stable isotope composition of outflow (lake)	%
E_s	enrichment slope	-

2.4 Model domain configuration and boundary conditions

2.4.1 Surface – subsurface flows

The HydroGeoSphere (HGS) modeling code (Aquanty Inc, 2023) was used to simulate the hydrological processes in the GGS Lake catchment. HGS is a 3-D, fully integrated, and physically-based model with the capacity to simulate the interwoven flow mechanisms of subsurface and surface water by coupling solutions obtained from the diffusion-wave of the two-dimensional, depth-integrated diffusion-wave of the Saint Venant equation governing surface water flow (Eq. 8, Viessman Jr. and Lewis, 1996) and the Richards' equation governing three-dimensional unsaturated and saturated subsurface flows (Eq. 9).

Eq. 7

$$\frac{\partial \phi_0 h_0}{\partial_t} - \frac{\partial}{\partial_x}\left(d_0 K_{0x} \frac{\partial h_0}{\partial_x}\right) - \frac{\partial}{\partial_y}\left(d_0 K_{0y} \frac{\partial h_0}{\partial_y}\right) + d_0\, \Gamma_0 \pm Q_0 = 0$$

ϕ_0 represents the porosity (dimensionless) of the surface flow domain, which varies based on the presence of rills and obstructions. h_0 stands for the water surface elevation (L). t denotes time (T). d_0 indicates the depth of flow (L). K_{0x} and K_{0y} represent surface conductance. Γ_0 is the water exchange rate ($L^3\ L^{-3}\ T^{-1}$) occurring between the surface and subsurface systems. Q_0 represents external sources or sinks.

The interaction between the two flow domains is facilitated by the exchange term Γ_0 through:

Eq. 8

https://doi.org/10.5194/hess-2024-214
Preprint. Discussion started: 9 September 2024

$$\boldsymbol{d_0 \,\Gamma_0 = \frac{k_r K_{zz}}{l_{exch}} (h - h_0)}$$

k_r symbolizes the exchange's relative permeability. K_{zz} represents the saturated hydraulic conductivity in the vertical direction. l_{exch} corresponds to the coupling length.

Eq. 9

$$\boldsymbol{\nabla . (W_m \, q) + \sum \Gamma_{ex} \pm Q = W_m \, (\frac{\partial}{\partial_t})(\theta_s S_w)}$$

In the given context: *Wm* (dimensionless) represents the volumetric porosity fraction within the porous media domain. Γ_{ex} stands for the volumetric exchange rate ($L^3 \, L^{-3} \, T^{-1}$) occurring between the porous media and other flow domains. *Q* denotes the source or sink term. *t* signifies time (T). θ_s corresponds to porosity (dimensionless). S_w refers to the degree of water saturation (dimensionless).

The flow rate *q* ($L \, T^{-1}$) is portrayed as:

Eq. 10

$$\boldsymbol{q = -K . k_r \, \nabla h}$$

K signifies the hydraulic conductivity ($L \, T^{-1}$). k_r represents the relative permeability (dimensionless), which is dependent on water saturation. *h* corresponds to the hydraulic head (L), calculated as the sum of the elevation head and pressure head.

The three-dimensional surface-subsurface flows in porous media and saturated zones were solved with the control volume finite element method. Nonlinear equations were linearized using Newton-Raphson and solved iteratively at each time step for the entire hydrologic system.

2.4.2 Evapotranspiration

The evapotranspiration process needs specific prerequisites for accurate parameterization as it is treated to play a dual role in the HGS as both a boundary condition and a distinct domain. Within this framework, the evapotranspiration fluxes encounter a restriction governed by a potential evapotranspiration flux (PET) which is defined by the modeler. The PET values are designated a boundary condition, serving its purpose on the surface domain. With each subsequent time step, a condition emerges, if the calculated actual evapotranspiration (AET)

https://doi.org/10.5194/hess-2024-214
Preprint. Discussion started: 9 September 2024

surpasses the PET, then the PET value is employed as a flux directed toward the relevant model faces. Conversely, if the calculated AET falls short of the PET, the computed AET value itself becomes the applied flux. Additional details on the evapotranspiration process formulations within the HGS model are presented in Kristensen and Jensen (Kristensen and Jensen, 1975). The two-dimensional PET database used in this research is calculated using the energy balance method and covers the period 2000 - 2022. The method is a balance of the energy terms which are the net radiation, the change in the heat content of the lake, and the latent and sensible heat fluxes. The equation is based on measurements of global radiation, air and water temperature, cloud cover, and vapor pressure. The latent heat flux, which represents the energy used for evaporation, was determined by subtracting the sensible heat fluxes and the change in the heat content of the lake from the net radiation. The evaporation rate was then calculated by dividing the latent heat flux by the latent heat of vaporization of the water. A maximum evaporation threshold of 15 mm/day was set. More details are given by Ölmez et al., 2024.

The simulation domain encompasses the entire GGS Lake catchment (Fig. 4) which is defined based on the surface topography considering the equipotential lines derived from the lakes' levels and measurements of the hydraulic head surrounding the lakes (piezometers). The surface topography across the catchment was produced by stitching a digital elevation model (DEM) from The Shuttle Radar Topography Mission (SRTM) with a resolution of 30 m, and the bathymetry data of GGS (Wolter, 2010) and Sacrow Lake (SAS) (Lüder et al., 2006, Bluszcz et al., 2008). Due to the high vegetation density, flat elevations, and the substantial hydraulic conductivity of the predominantly sandy soil, the absence of river formation is currently observed in the catchment. The foundational 2-D triangular mesh supporting the comprehensive 3-D triangular prism grid within the HGS model was created using AlgoMesh (Merrick, 2017). Each 2-D mesh layer encompasses a total of 2837 mesh nodes and 5300 triangular finite elements (Fig. 4). The complete 3-D model (Fig. 4) grid extends the 2-D mesh across 15 subsurface layers, broadly categorized as one soil layer, 14 Quaternary material layers, and one competent bedrock layer (Rupel clay).

https://doi.org/10.5194/hess-2024-214
Preprint. Discussion started: 9 September 2024

Hydrology and Earth System Sciences
Open Access
Discussions

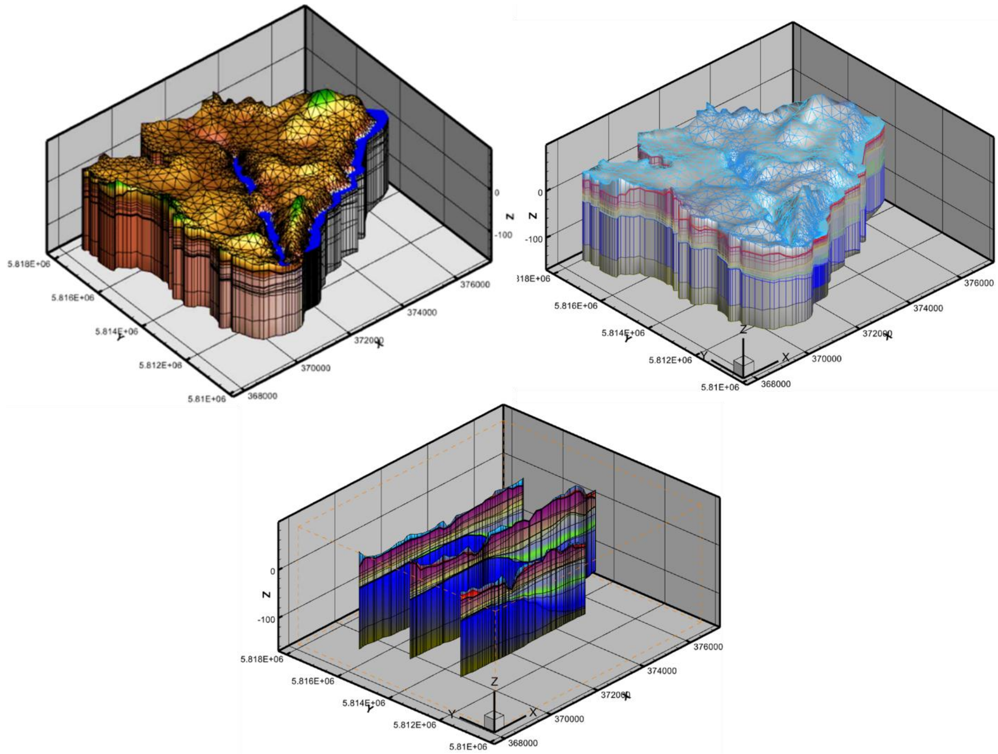

Fig. 4. Hydrostratigraphic units and enlarged view of the mesh within the Gross Glienicke Lake catchment

Spatially distributed land cover data (Fig. 1) were utilized to capture a broad range of factors influencing evapotranspiration and overland flow, including evaporation depth, root depth, leaf area index (LAI), surface roughness, rill storage height, and obstruction storage height. Specific parameters for evapotranspiration (ET) and overland flow are tailored to each land cover type. To accurately reflect the impact of vegetation growth on water demand through evapotranspiration, the Leaf Area Index (LAI) during winter (January) and summer (July) using the Sun Sacan device type SS1 were measured, capturing both maximum and minimum current LAI values. The measured LAI indices were then compared with data from the MCD15A2H Version 61 Moderate Resolution Imaging Spectroradiometer (MODIS), which provides a 4-day composite with a pixel size of 500 m for January and July (Myneni et al., 2021). Corrected monthly average MODIS LAI values for each land cover type, spanning from 2000 to 2023, were subsequently integrated into the HGS model.

2.4.3 Unsaturated zone

https://doi.org/10.5194/hess-2024-214
Preprint. Discussion started: 9 September 2024

The top subsurface layer in the 3-D mesh with spatial varying depths shows the distribution of soil materials across the catchment. The soil data were obtained from the soil map with a scale of 1:200,000 (BUEK200) which was prepared by the Federal Institute for Geosciences and Natural Resources (BGR, 2007). The soil samples were collected from various depths, extending up to 3 meters, at 10 different sites, primarily in the groundwater recharge area (Döberitzer-Heide region) and natural conservation zones. The sampling locations were selected based on soil types. The percentages of sand, silt, and clay for each soil type were determined in the laboratory to classify the soil textural types, using the United States Department of Agriculture (USDA) soil textural calculator. A set of 2 soil textural types, sand, and loamy sand has been recognized. Unsaturated soil hydraulic parameters and soil moisture retention properties required for the van Genuchten application with the HGS model were uniquely estimated for each soil type using the ROSETTA program, version 1 (Schaap et al., 2001).

Underlying the soil layers are 14 Quaternary geology layers that overlie bedrock. To represent the topography of the subsurface in the lake catchment, relevant data was extracted from the groundwater model provided by Berliner Wasserbetriebe. This model (software FEFLOW) was calibrated in 2012 and updated in 2013 (BWB, 2012 and 2013) using measured data from the year 2010. The model focuses on analyses of the waterworks at Beelitzhof, Tiefwerder, and Kladow. It, therefore, covers areas along both banks of the river Havel. Additional datasets from boreholes were merged into a single surficial geology dataset using the Rockware model setup for the GGS Lake catchment (Hermanns, 2022). The initial hydraulic conductivity values for each type of Quaternary material were taken from the FEFLOW model. The hydraulic properties of the unsaturated zone were manually adjusted during manual model calibration.

2.4.4 Groundwater – lake levels loggers

A total of 8 groundwater monitoring wells scattered within the catchments, along with two loggers set on the lakes, provide a well spatially distributed dataset of groundwater-lake level dynamics for evaluating model simulations. The groundwater monitoring wells were selected based on location, catchment area, and data availability spanning from 2000 to 2023. GGS has been monitored since 1964. Moreover, within the study catchment, the regulated flow system of the river Havel is maintained to facilitate water conveyance. Since 1980, an established logger has been operational to meticulously monitor the water level dynamics within this river. For the presented study particular interest lies in loggers No. 51, 52 (WD-

https://doi.org/10.5194/hess-2024-214
Preprint. Discussion started: 9 September 2024

GGS and WS-GGS), and 3154 (E-GGS). WD-GGS(50) and WS-GGS(51) belong to two different aquifers (shallow(WS-GGS) and deep aquifer (WD-GGS) and are situated on the western side of GGS (Brandenburg, Fig. 3). These loggers in the recharge area of the GGS lake consistently maintain water levels averaging 15-20 cm higher than the GGS. Additionally, logger E-GGS, located close to the eastern shoreline downstream of GGS (Berlin), consistently registers water levels averaging 30-40 cm lower than the GGS lake (Fig. 3).

2.4.5 Groundwater abstractions

Two major drinking water supply systems, Kladow and Beelitzhof, located alongside Havel on the southwest side of Berlin have been in operation since 1888 and 1932 respectively by BWB. Kladow comprises 16 wells up to 93 meters deep and a maximum pumping rate of 30,000 m^3/day, while Beelitzhof has 85 wells up to 170 meters deep and a maximum pumping rate of 160,000 m^3/day. To assess the impact of groundwater withdrawals from deeper layers, the model domain was extended to a depth of 150 meters below sea level. According to studies BWB, upto 80 percent of the water extracted by Kladow originates from bank filtration along the river Havel. The remaining 20 percent of the extracted water originates directly from groundwater recharge as well as outflow from GGS. As various water resources contribute to the overall drinking water production in the main waterworks in this area (Beelitzhof, located on the western side of the Havel), a detailed analysis was conducted to assess the share of the GGS Lake catchment. The analysis involved the implementation of distinct scenarios within the hydrologic model.

2.4.6 Model evaluations

This study emphasizes the importance of a multifaceted approach to evaluate hydrological model performance, utilizing both traditional and innovative methodologies. Initially to evaluate model performance the simulated seasonal and long-term groundwater and lake level fluctuations will be compared to observed water levels of the lakes and piezometers around the lakes. The performance evaluation of hydrological models commonly relies on various metrics such as the Nash-Sutcliffe efficiency (NSE), percent bias (PBIAS), root mean squared error (RMSE), and the Kling-Gupta efficiency (KGE). The KGE, introduced by Gupta et al. (2009), offers a comprehensive assessment by considering bias, correlation, and variability separately. Given the specific hydrological focus of each metric, a multi-metric approach was adopted for calibrating the HGS model parameters, as demonstrated to efficiently balance

https://doi.org/10.5194/hess-2024-214
Preprint. Discussion started: 9 September 2024

model performance by previous studies (Pfannerstill et al., 2014; Mahmoodi et al., 2020). For model assessment, NSE, PBIAS, RMSE, and KGE were employed as performance metrics on a monthly basis. Calibration runs were evaluated based on predefined thresholds for NSE (0.65), PBIAS (-25% to 25%), and KGE (0.65) to identify the most suitable configurations. The calibration process was carried out manually due to the model's long execution time and limited computational capacity. Emphasis was placed on calibrating model parameters of the unsaturated zone which governs water movement into the soil and subsequently into or out of the aquifer. The initial hydraulic conductivity values for each type of soil were determined from existing literature (Steidl et al 2023) and lab analysis and later manually adjusted during model calibration. The model parameterization for the saturated zone was initially derived from the FEFLOW model calibrated by the BWB (BWB, 2012/2013). The calibration and validation periods chosen for the simulation runs were 2008-2018 and 2019–2023, respectively, preceded by an eight-year spin-up phase before 2008 to reach quasi-steady state condition fitting to the conditions in 2008.

To evaluate the performance of the HydroGeoSphere (HGS) model on different angles, a detailed assessment involving the simulation of the inflow to GGS Lake (denoted as I_{HGS}) was undertaken. This parameter (I_{HGS}) was subsequently used as a testing parameter to evaluate the model's performance in calculating evaporation rates for the years 2022 and 2023 using an independently determined E/I ratio. The evaporation rate (E_{ISO}) can be expressed as:

Eq. 11

$$\boldsymbol{E_{ISO} = \frac{1}{A} . I_{HGS} . P}$$

Where A is the area of the lake water body (m^2), I_{HGS} represents the annual inflow to the lake (m^3) and *P* is the percentage of losses of inflow due to evaporation derived from the isotope analysis (*E/I*). Figure 5 shows the methodology used to evaluate the model performance across different dimensions. The underlying assumption for this evaluation is that an accurate simulation of inflow to the lake by the HGS model (I_{HGS}) would yield evaporation rates (E_{ISO}) comparable to those calculated by the HGS model (E_{HGS}). Thus, the consistency between evaporation estimates derived from both approaches serves as a validation of the HGS model's capability to simulate other water balance components precisely.

https://doi.org/10.5194/hess-2024-214
Preprint. Discussion started: 9 September 2024

Hydrology and Earth System Sciences
Open Access
EGU
Discussions

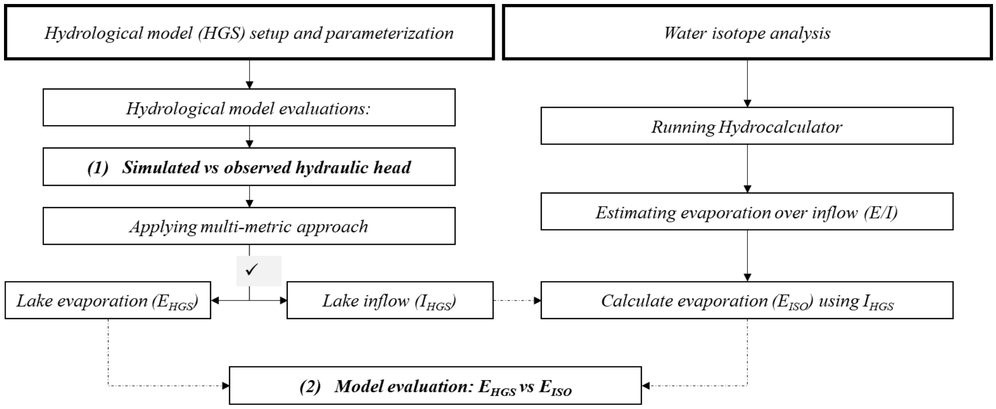

Fig. 5. Flow chart of the methodology employed to evaluate the model performance

The well-captured inflow and subsequent evaporation rates for the years 2022 and 2023 by the HGS model, allow us to extend this approach for estimating evaporations during the earlier period from 2015 to 2021. This period is crucial as it encompasses years without water isotope analyses, during which significant drops in lake and groundwater levels were observed. However, the E/I ratio derived from recent years (2022 and 2023) cannot be directly applied to earlier years due to variations in temperature and inflow, which are key factors influencing isotopic signatures (dilution and enrichment). To adjust the E/I ratio for earlier years, we incorporated annual temperature variations and inflow data into our model. Specifically, we compared the temperature and inflow of each specific year ($_{Yx}$) to the corresponding values from 2022 and 2023($_{Y22\text{-}23}$). This comparison yielded ratios for temperature ($T_{Yx}/T_{Y22\text{-}23}$) and inflow (I_{Y2023}/I_{Yx}), which were used to modify the E/I ratio accordingly. For instance, to apply the $E/I_{Y22\text{-}23}$ to the year 2015, we multiplied the $E/I_{Y22\text{-}23}$ ratio by the temperature ratio ($T_{Y15}/T_{Y22\text{-}23}$) and the inflow ratio ($I_{Y2023}/I_{Y15}$). A temperature ratio greater than 1 indicates higher temperatures in 2015 compared to 2023, suggesting a higher E/I ratio, greater evaporation, and enrichment. An inflow ratio greater than 1, indicating lower inflow in 2015 compared to 2023, would lead to a greater E/I ratio, reflecting greater evaporation and enrichment. The adjusted E/I ratios were then applied to refine the initial evaporation estimates from the isotopic mass balance model. These revised evaporation estimates were subsequently compared to the evaporation rates calculated by the HGS model for the period 2015-2021.

3. Results

https://doi.org/10.5194/hess-2024-214
Preprint. Discussion started: 9 September 2024

Isotopic analysis

Alterations in the mean monthly isotopic compositions of lake water and groundwater, along with temperature and precipitation data, from August 2022 to August 2023 is presented in Figure 6. The δD values for GGS (Fig. 6a), show significant variability, showing a pronounced drop in δD values from around -8‰ in August 2022 to -17‰ in January 2023, followed by a gradual decrease (except February) to approximately -16‰ by June 2023, which represent a strong dilution phase. The period from July to September demonstrates enriched values of δD alongside rising temperature and evaporation as a consequence. The δ^{18} O values for GGS (Fig. 6b) record a fluctuating pattern, ranging from -0.27‰ to 1.4‰, with peaks observed in August 2022 and July 2023, but experienced noticeable drops in April and May 2023. Overall, the isotopic data indicate that GGS experiences great isotopic enrichment (heavier isotopic composition).

The δ^2H values of groundwater on the east side of GGS (E-GGS, Fig. 6c) range from approximately -40‰ to -50‰, with notable fluctuations throughout the year. The isotopic composition of groundwater on the west side of GGS (W-GGS, Fig. 6c) has less variability, with δD values mostly remaining between -55‰ and -60‰, suggesting a rather stable isotopic environment. Despite the fluctuations in δD values, the δ^{18}O values (Fig. 6d) show less variation, indicating some degree of isotopic stability in the oxygen isotopes in the groundwater of both sides of lakes. E-GGS presents a relatively stable trend with δ^{18}O values fluctuating between -5‰ and -6‰. W-GGS, with a seasonal pattern similar to E-GGS, shows a consistent range of δ^{18}O values between -8‰ and -8.5‰ with minimal fluctuations (Fig. 6d). Overall, the E-GGS with heavier isotopic signatures experiences greater isotopic variability, meanwhile, the W-GGS site maintains a more consistent isotopic signature, indicative of a more stable hydrological regime. These observations (Fig. 6a,b,c,d) indicate that the isotopic composition of both lake water and groundwater was generally heavier (stronger enrichments) during the summer of 2022 compared to the summer of 2023.

The monthly average temperature (TMP, Fig. 6e), follows a clear seasonal pattern. It drops from around 20°C in August 2022 to a low of 5°C in January 2023, then rises again to about 20°C by July 2023. Alongside temperature, precipitation values fluctuate significantly, with peaks exceeding 90 mm in August 2022 and June 2023, and lower values around 20 mm observed in Oct and November 2022 and May and Septemeber 2023.

https://doi.org/10.5194/hess-2024-214
Preprint. Discussion started: 9 September 2024

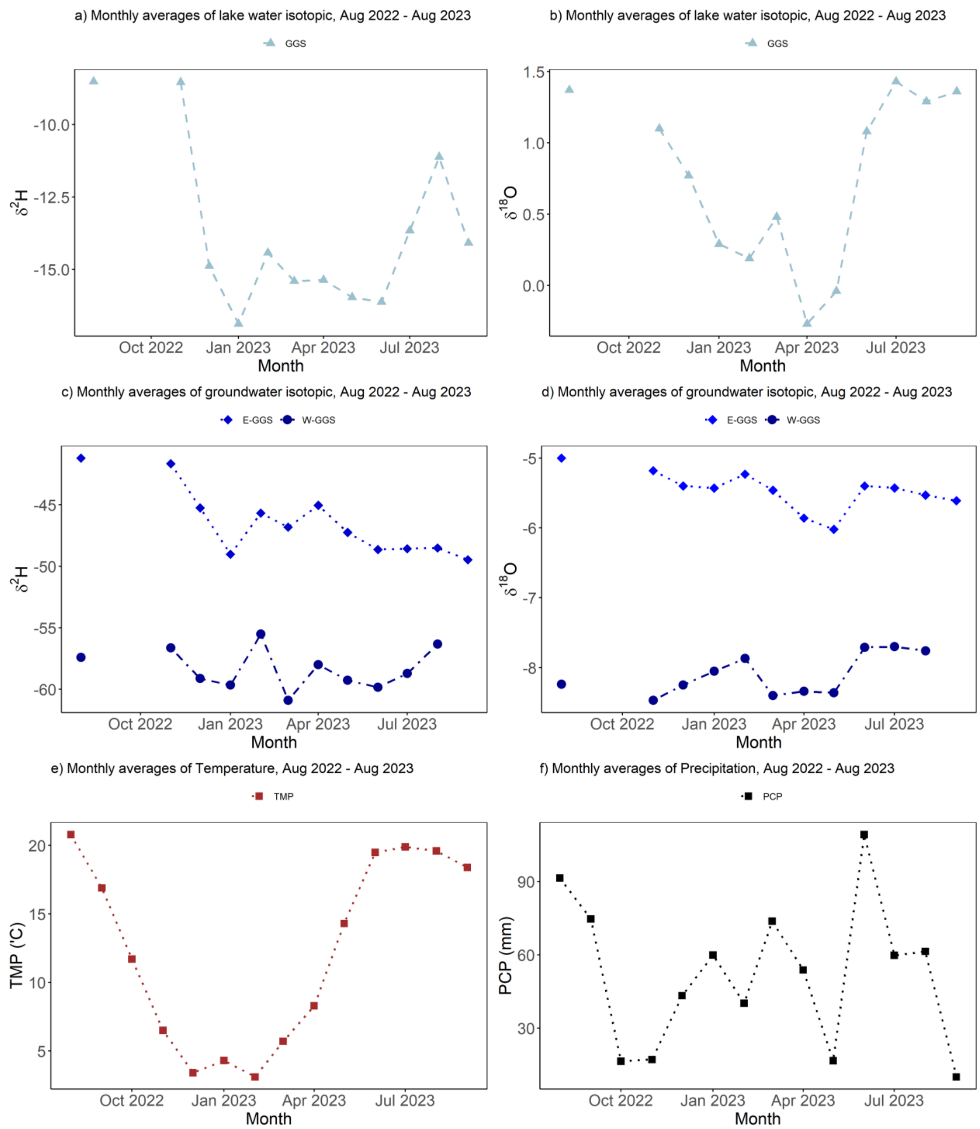

Fig. 6. Monthly averages of lake water isotopic compositions (a: δD and b: δ^{18}O), groundwater isotopic compositions (c: δD and d: δ^{18}O), temperature (e), and precipitation (f) data from August 2022 to September 2023.

The relationship between δD and δ^{18}O values for lake water (GGS) and groundwater (WGGS and EGGS) from August 2022 to September 2023 are illustrated in Figure 7. The isotopic values for lake water are significantly clustered, with δD values between -25‰ and -5‰ and δ^{18}O values from 2‰ to -2‰ and are isotopically heavier compared to precipitation and groundwater, suggesting significant evaporative enrichment. WGGS exhibits δ^2H values from

-50‰ to -65‰ and $\delta^{18}O$ values from -9‰ to -7‰. EGGS δ^2H values range from approximately -50‰ to -40‰, with $\delta^{18}O$ values between -7‰ and -5‰, indicating less enrichment compared to lake water and higher enrichment compared to the groundwater on the west side.

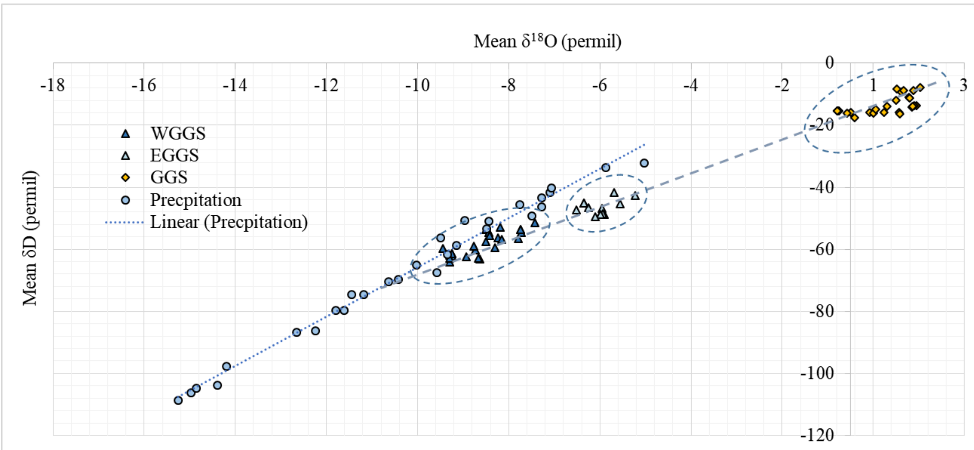

Fig. 7. Isotopic composition of lake water and groundwater measured on the west (WGGS) and east (EGGS) sides of Groß Glienicke from August 2022 to September 2023. The local meteoric water line (LMWL) is driven from (GNIP/Berlin (DWD, BFG, BGR & HHZM, Stumpp et al. 2014).

Variables used for the calculation of evaporative losses and evaporation over inflow ratio (E/I) ratios calculated for GGS during the August 2022–September 2023 period are presented in Table 2. The winterwater isotopic compositions (dilution phase) served as the initial sampling point for calculating the E/I ratio in both years 2022 and 2023. The δ_A-value of the ambient air moisture was calculated based on the stable isotope composition of local precipitation sampled in the Groß Glienicke region and the Lankwitz campus of the Freie University Berlin. The calculated evaporative losses over inflow were equal to 43.4% and 42.3% based on δD and 30.11% and 29.4% based on $\delta^{18}O$ in 2022 and 2023 respectively. The E/I ratio calculated based on δD is around 12% higher compared to the E/I based on $\delta^{18}O$. Therefore, as a mean ratio, an average of 37% will be used for furhter analyses.

Table 2. Variables used for calculation of evaporative losses and the ratio of total evaporation to inflow (E/I) as a function of the measured δD and $\delta^{18}O$ isotope enrichments for Lake Gross Glienicke (GGS) surveyed during the August 2022–September 2023.

https://doi.org/10.5194/hess-2024-214
Preprint. Discussion started: 9 September 2024

Parameters	Description	δD	$\delta^{18}O$
ε□	Kinetic isotope fractionation factor [‰] (h dependent)	-887.5	-1008.2
ε*	Equilibrium isotope fractionation factor [‰] (T dependent)	78.7465	9.3468
ε	Total isotope fractionation [‰]	-814.5018	-998.9398
Ck	Kinetic isotope fractionation constant [‰]	12.5	14.2
α*	Equilibrium isotope fractionation factor [‰] (T dependent)	1.0787	1.0093
δ*	Limiting isotope composition	-134.7724	-30.2151
m	Enrichment slope	-1.0129	-1.0138
δ_A	Ambient air moisture	-124.9844	-16.7601
E/I_{Y2022}	Evaporation over inflow ratio [‰] of Groß Glienicke Lake in 2022	43.37	29.63
E/I_{Y2023}	Evaporation over inflow ratio [‰] of Groß Glienicke Lake in 2023	42.28	29.07

Hydrological modeling and model evaluations

Figure 8 illustrates the simulated vs. observed hydraulic heads (meters above sea level: m a.s.l.) at West-GGS Piezometer (W-GGS), Lake Gross Glienicke (GGS), and East-GGS Piezometer (E-GGS) over the period from January 2008 to December 2023. The model's performance is evaluated using several metrics, including the Kling-Gupta Efficiency (KGE), Percent Bias (PBIAS), and Root Mean Square Error (RMSE), as shown in Table 3. A strong alignment is evident between simulated and observed hydraulic heads, both in terms of magnitude and seasonality.

The simulated groundwater levels on the west side of the lakes, despite some over- and underestimations, showed very good agreement with the observed data. For the calibration period (2008-2018), the performance metrics are KGE of 0.86, PBIAS of 0.0%, and RMSE of 0.13 m. During the validation period (2019-2023), the model maintained high performance with a KGE of 0.82, PBIAS of -0.1%, and RMSE of 0.07 m. Both observed and simulated data exhibit a general declining trend over the study period, with hydraulic heads decreasing from approximately 30.15 m to 30 m.

For GGS, similar to W-GGS, both observed and simulated values show a decreasing trend from around 31 m in 2008 to approximately 29.80 m in 2023. The model simulations closely follow the observed data, with minor deviations. The performance metrics for GGS during the calibration period are KGE of 0.78, PBIAS of -0.2%, and RMSE of 0.13 m. In the validation period, the metrics are KGE of 0.75, PBIAS of 0.0%, and RMSE of 0.06 m, indicating high accuracy in representing the hydraulic behavior of the lake.

The observed and simulated groundwater dynamics on the east side of GGS show good agreement. During the calibration period, the performance metrics are KGE of 0.84, PBIAS of 0.1%, and RMSE of 0.09 m. In the validation period, the metrics are KGE of 0.70, PBIAS of 0.2%, and RMSE of 0.09 m. Overall, the high-performance metrics confirm the model's reliability and accuracy in capturing both the long-term trends and seasonal variations of groundwater-surface water dynamics within the study area, providing valuable insights into groundwater-surface water interactions.

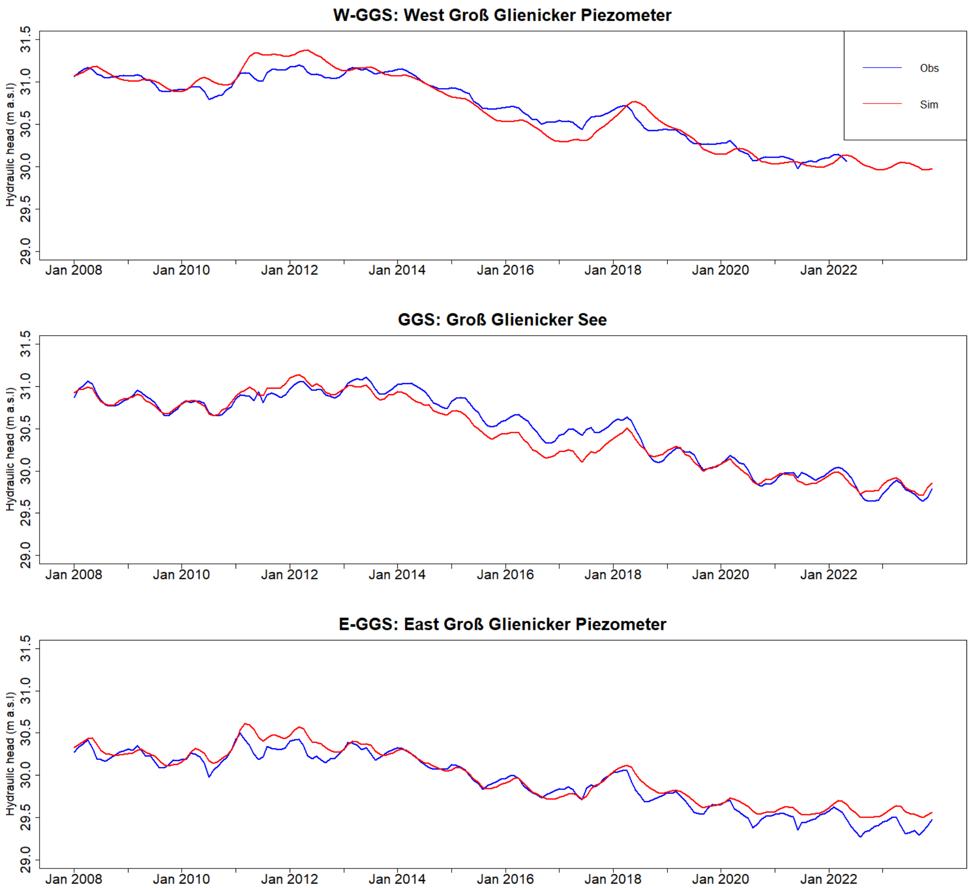

Fig. 8. Time series of observed and simulated hydraulic heads at three locations: (a) West Gross Glienicke Piezometer (W-GGS), (b) Lake Gross Glienicke (GGS), and (c) East Gross Glienicke Piezometer (E-GGS) from January 2008 to December 2023.

Table 3. Model performance evaluation using several metrics for both calibration (2008-2008) and validation (2018-2023) periods

		West Gross Glienicke	East Gross Glienicke	Gross Glienicke Lake
Calibration	**KGE**	0.86	0.84	0.78

https://doi.org/10.5194/hess-2024-214
Preprint. Discussion started: 9 September 2024

2008-2018	**PBIAS**	0.0	0.1	-0.2
	RMSE	0.13	0.09	0.13
Validation 2019-2023	**KGE**	0.82	0.7	0.75
	PBIAS	-0.1	0.2	0
	RMSE	0.07	0.09	0.06

The calculated annual water exchange for GGS from 2008 to 2023, detailing the inflow to the lake, outflow from the lake, and their differences (net flow = inflow - outflow) are presented in Figure 9. The inflow to GGS demonstrates substantial annual variability. For instance, years such as 2008, 2011, 2012, and 2018 show relatively higher inflows compared to other years. Notably, there is a discernible decreasing trend in inflow from 2011 to 2021, with 2018 being an exception. This trend indicates a progressive reduction in the hydrological inputs to the lake over the decade. Simultaneously, the outflow from GGS shows significant annual variability, with the highest outflow occurring between 2012 and 2017. This increased outflow, coupled with the decreasing inflow, points to a period of significant net water loss for GGS, potentially impacting the lake's water levels. Positive net flow values in years 2011, 2018, and 2022 indicate years when inflow exceeds outflow, contributing to the lake's water gain. Variation in both water gain and loss over the study period, reflects the complex interplay of natural hydrological processes governing the lake's water balance.

Figure 10 illustrates the water exchange dynamics of GGS over the period from August 2022 to September 2023, highlighting seasonal patterns in inflow, outflow, and net flow. During the warmer months, particularly June and July, the inflow to the lake peaks at approximately 90,000 m^3, indicating a significant increase in water input during this period. Among the summer months (July to September), August has the lowest amount of inflow, with an average of approximately 40,000 m^3. In contrast, the inflow is pronouncedly lower during the months of March, April, and May, averaging around 20,000 m^3. The lake experiences positive net flow, reflecting water gain, during the months of June and July. From December to May (except February), the net flow is predominantly negative, indicating that outflow exceeds inflow. During these months, the lake loses water, with outflow reaching its highest levels.

https://doi.org/10.5194/hess-2024-214
Preprint. Discussion started: 9 September 2024

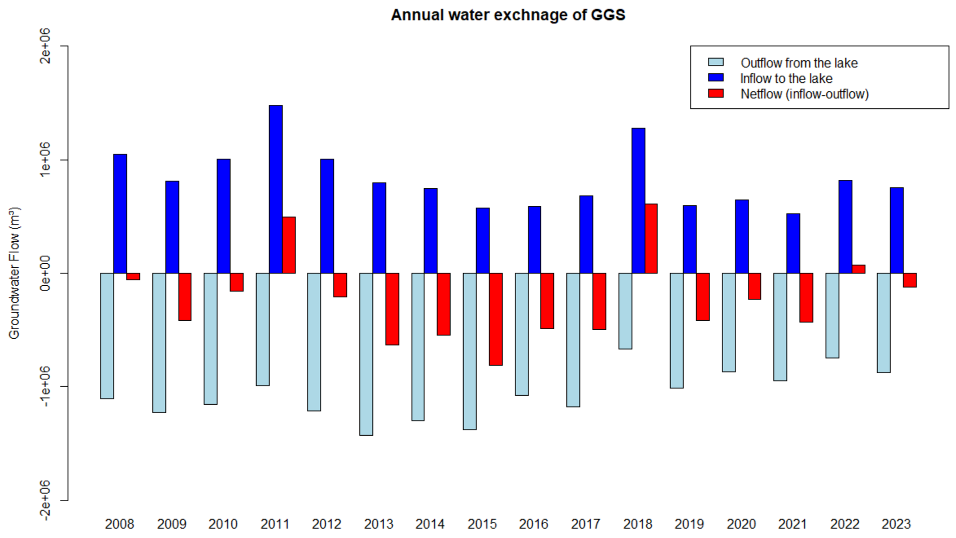

Fig. 9. Annual water exchange of Lake Groß Glienicke (GGS) from 2008 to 2023, showing the inflow to the lake, outflow from the lake, and net flow (Outflow - Inflow)

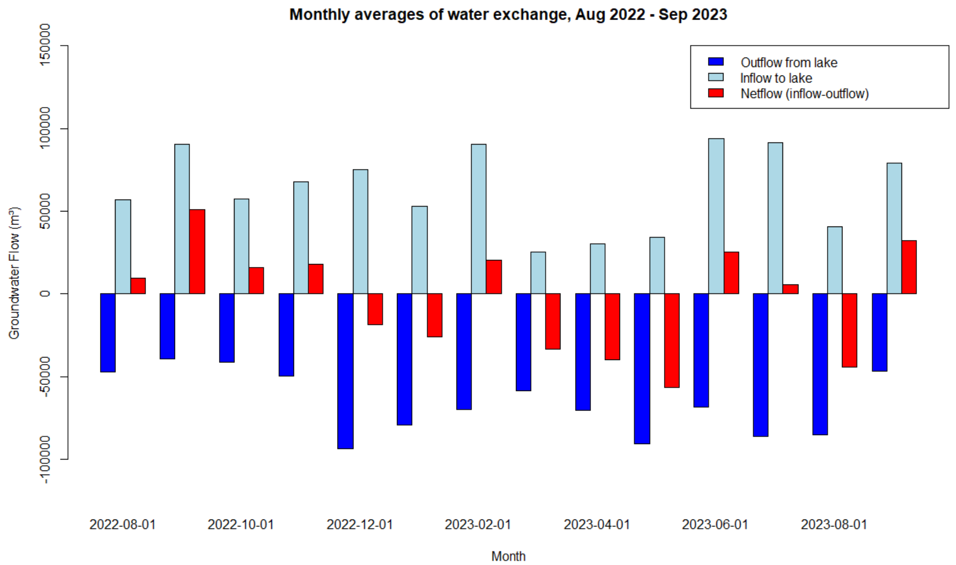

Fig. 10. Monthly water exchange of Lake Gross Glienicke (GGS) from August 2022 to September 2023

https://doi.org/10.5194/hess-2024-214
Preprint. Discussion started: 9 September 2024

To compare the lake evaporation values calculated by the HGS model and the results of the isotopic signature of lake water actual evaporation (E) from GGS for the years 2022 and 2023 was calculated using Eq. 11, which incorporates simulated annual water inflow to GGS (I_{HGS}) from the HGS model and the E/I ratio derived from isotope analysis (mean ratio: 37%). These results were compared to the evaporation rates from GGS simulated by the HGS model (Fig. 11). The annual evaporation estimates from the isotope analysis for the years 2022 and 2023 show good agreement. The values calculated by the HGS model (E_{HGS}) are slightly lower (around 80 mm). The general agreement between the evaporation rates simulated by the HGS model and the values derived from the isotope approach indicates accurate inflow simulation by the HGS model. Transferring the *E/I* ratios from 2022 and 2023 to calculate evaporation for earlier years (2015-2021, Fig. 11) results in notable discrepancies, particularly evident in 2015 and 2018, where evaporation reaches 450 and 1000 mm, respectively, compared to E_{HGS} values of 590 and 614 mm for those years. However, modified isotope analysis (considering annual variations in inflow and temperature, see Eq.11) demonstrates good agreement with the HydroGeoSphere model, emphasizing our approach of incorporating temperature and inflow data for accurate evaporation predictions for earlier years. This suggests that while the *E/I* ratio obtained from 2022 and 2023 can be applied to estimate evaporation in previous years, adjustments for differences in inflow and temperature between those years and 2022-2023 are crucial for enhanced estimations of evaporations in years without isotope analysis (E/I).

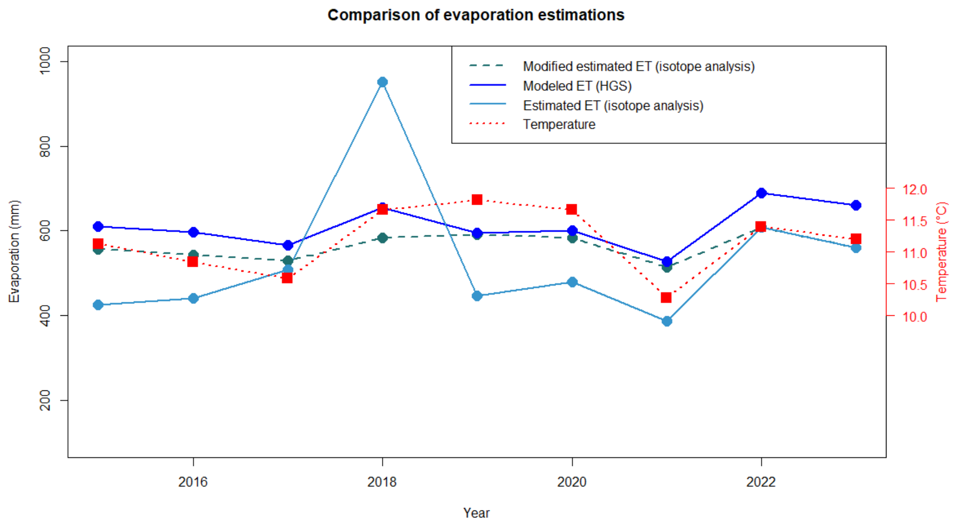

Fig. 11. Comparison of actual evaporation from Lake Gross Glienicke (GGS) estimated by Hydroeosphere model (HGE) and isotope analyses (E/I ratio), and modification of isotope analyses (E/I ratio) considering annual temperature and inflows to the lake. Annual temperatures are indicated, corresponding to the secondary y-axis.

4. Discussion

The comparison of actual evaporation (E) from GGS for 2022 and 2023, derived from isotope analysis (E/I) and HydroGeoSphere (HGS) model calculations, demonstrates the comparability of these methods. Despite slight differences in the results, likely due to the influence of direct precipitation with lighter isotope signatures diluting the lake water, the general consistency between the methods underscores the accurate simulation of inflows by the HGS model. Seasonal variations in water isotopic compositions offer a valuable perspective for evaluating hydrological model simulations. Higher outflow observed from December 2022 to May 2023 provides insights into the dilution phase of groundwater isotopic compositions on the eastern side of GGS during these months. Notably, GGS water isotopes reached their heaviest form in August 2023, contrasting with other summer months with similar temperatures and precipitation, suggesting lower inflow during that particular month as simulated by the HGS model. This approach highlights the value of using isotopic data to evaluate model simulations, providing a complementary angle to traditional methods. Considering the higher precipitation and warmer temperatures in the summer of 2022 compared to the summer of 2023, the isotopic composition of both lake water and east groundwater was heavier during the summer of 2022. This indicates that isotopic "light" rainwater, which directly recharged the lakes in the summer of 2022, was insufficient to counterbalance the influence of the higher temperatures, resulting in a heavier isotopic composition in the lakes. Despite the high precipitation in summer 2022, which would typically dilute the isotopic signature of the lake, the higher temperatures (evaporation) led to an enrichment of water isotopes. This phenomenon can be attributed to the large water body of the lake (approximately 4 million m³ considering the average water depth of 6.5 m reported by Wolter and Ripl (1999) compared to the rain amount (0.05 million m³), where the relatively small volume of rainwater was not enough to significantly alter the isotopic composition of the much larger lake volume. This is in line with the findings of the study by Vyse et al.2020 where they discovered a more significant influence of rain on shallow water bodies compared to larger water bodies in the State of Brandenburg (NE-Germany). The low impacts of rainwater on the isotope composition of the lake can also be interpreted to mean that GGS is a groundwater-dominated lake with a very good hydraulic connection to the groundwater, which keeps the lake water fresh and diluted by providing a source of isotopically-depleted water. This underlines the robustness of the isotopic approach against the variations of meteorological factors influencing the isotopic signature.

The isotopic differences between lake water and groundwater on both side of the GGS, highlight the complex interactions and distinct hydrological processes occurring within the study area. Considering that the groundwater samples from the east and west of GGS belong to the same depth (9-10 m below surface) and same aquifer, the isotopically-enriched groundwater in the east side can only be explained by a well-mixed interaction of lake water and groundwater in this area. This underlines that GGS is a flow-through lake, a conclusion supported by the E/I ratio being up to 37% (e.i., mean ratio) in 2022 and 2023. The E/I ratio of GGS aligns with the E/I ratio reported for wetlands and lake water bodies downstream of the Spree catchment showing similar climate conditions. In 2021, the E/I ratio in this area was up to 34% (Chen et 625 al., 2023). Vyse et al. (2020) reported that the wetlands with lower landscape elevations located in northen Brandenburg typically possessed higher E/I ratios than the ones with higher elevations. This is due to the hydrological function of small waterbodies in the Pleistocene landscape. Higher wetlands have a more recharge/flow through character whereas lower positions show a discharge character. Moreover, Cluett and Thomas (2020) highlighted that the sensitivity of lake water isotopes to inflow and evaporation can vary significantly over time, influenced by regional hydroclimate (e.g., direct precipitation and humidity) and local hydrology (e.g., type of the lake). The uncertainty in

https://doi.org/10.5194/hess-2024-214
Preprint. Discussion started: 9 September 2024

evaporative loss calculated using the code embedded in the Hydrocalculator is mainly due to uncertainties in the required inputs, temperature, and humidity, which can cause variations of up to 2% (E/I) according to Skrzypek et al. (2015). Despite these potential measurement variations, the calculated E/I ratio for GGS provides a reliable estimate that aligns with known hydrological behaviors in similar regions.

For the period 2015-2021, evaporation estimates derived from the isotope analysis (E/I) of 2022 and 2023 generally show lower values compared to the HGS model's evaporation estimates, except 2018. This year saw a strong inflow peaking due to heavy rainfall events in the summer 2017. This suggests that using the E/I ratios from 2022 and 2023 for earlier years without adjustments can lead to significant inaccuracies. The modified isotope analysis (E/I), which incorporates annual variations in inflow and temperature, shows a better agreement with the HGS model evaporation calculates, especially in the earlier years. This finding underscores the importance of including both temperature and inflow data for more accurate evaporation predictions. Comparing these results with previous studies, Herbst and Kappen (1999) reported evaporation from the Bornhöved Lake, which covers 1.1 km² in northern Germany and has a maximum depth of 26 m, to be around 650 mm for the years 1992-1995. The evaporation estimates for GGS from both the HGS model and the modified isotope analysis fall within a similar range reported by Herbst and Kappen (1999), suggesting that despite differences in geographical and hydrological characteristics, the annual evaporation rates for German lowland lakes are comparable. These findings support the use of comprehensive, multi-faceted approaches in hydrological studies to improve the precision of evaporation estimates and enhance water resource management.

5. Conclusion

This study has addressed the challenge of accurate estimation of water balance components comprehensively through the quantification of subsurface-groundwater inflow and evaporation losses to Gross Glienicke Lake (GG), located in northeast Germany. Through the combined use of the isotopic mass balance model, HydroCalculator, alongside the fully integrated hydrological model, HydroGeoSphere (HGS), a detailed understanding of the hydrological dynamics governing GG Lake was attained. The calculated evaporation rates derived from the isotopic mass balance model, exhibit strong alignment with the actual evaporation rates calculated by the HGS model. This alignment underscores on one hand the reliability and efficacy of the integrated hydrologic modeling approach in predictions of water balance components such as inflow to the lake in a complex hydrogeological setting. On the other hand, incorporating evaporation rate estimations given by isotope analysis corrected by temperature variations and historical inflows leads to an improvement of the inflow results even for the years without measured isotope data. Despite inherent uncertainties associated with water isotope signature analyses, the integration of isotopic data with hydrological modeling has provided valuable validation for the estimation of water balance components. Moving forward, this integrated approach holds promise for enhancing the robustness of hydrological models and facilitating more accurate assessments of water resources and ecosystem dynamics in similar lake environments.

Data availability: All data (except the data provided by Berliner Wasserbetriebe) used to process and set up the models will be available upon request. Data provided by Berliner Wasserbetriebe can be requested through a separate usage agreement with Berliner Wasserbetriebe.

Author contributions: Data collection, fieldwork, HGS model setup, and code development, model input-output analysis, writing (original draft, review, and editing). JS: Isotopic laboratory analysis, writing (review and editing). MS: Model input-output analysis, writing (original draft, review, and editing). CM: Model input-output analysis, writing (original draft, review, and editing).

Competing interests: The authors declare that they have no conflict of interest.

Acknowledgments: This investigation was funded through the Einstein Research Unit ‘Climate and Water under Change’ from the Einstein Foundation Berlin and Berlin University Alliance (ERU-2020-609). We would like to thank Reinhard Hinkelmann, Franziska Tügel, and Can Ölmez from the Technical University of Berlin for providing potential evaporation data. We like to thank Dr. Gunnar Lorenzen and Bertram Monninkhoff (Berliner Wasserbetriebe) for providing us with the FEFLOW model as well as the actual data on the drinking water extraction rates around the Havel River. We are grateful to our colleague, Dieter Scherer his rainwater sampling assistance, and Patrick Zentel for his field and laboratory assistance.

References

Ala-aho, P., Rossi, P.M., Isokangas, E. and Kløve, B., 2015. Fully integrated surface–subsurface flow modelling of groundwater–lake interaction in an esker aquifer: Model verification with stable isotopes and airborne thermal imaging. Journal of Hydrology, 522, pp.391-406.

Allison, G.B. and Leaney, F.W., 1982. Estimation of isotopic exchange parameters, using constant-feed pans. Journal of Hydrology, 55(1), pp.151-161.

Aquanty Inc., 2023. HydroGeoSphere: A three-dimensional numerical model describing fully-integrated subsurface and surface flow and solute transport. Waterloo, Ontario, Canada. https://www.aquanty.com/hgs-download.

Berliner Wasserbetriebe – BWB., 2012. Assessing the waterworks of Beelitzhof, Tiefwerder, and Kladow impacts on groundwater model using FEFLOW model, Unpublished.

Berliner Wasserbetriebe – BWB., 2013. Assessing the waterworks of Beelitzhof, Tiefwerder, and Kladow impacts on groundwater model using FEFLOW model, Unpublished.

Bluszcz, P., Kirilova, E., Lotter, A.F., Ohlendorf, C. and Zolitschka, B., 2008. Global radiation and onset of stratification as forcing factors of seasonal carbonate and organic matter flux dynamics in a hypertrophic hardwater lake (Sacrower See, Northeastern Germany). Aquatic Geochemistry, 14, pp.73-98.

Chen, K., Tetzlaff, D., Goldhammer, T., Freymueller, J., Wu, S., Smith, A.A., Schmidt, A., Liu, G., Venohr, M. and Soulsby, C., 2023. Synoptic water isotope surveys to understand the hydrology of large intensively managed catchments. Journal of Hydrology, 623, p.129817.

Cluett, A.A. and Thomas, E.K., 2020. Resolving combined influences of inflow and evaporation on western Greenland lake water isotopes to inform paleoclimate inferences. Journal of Paleolimnology, 63(4), pp.251-268.

DWD, C.D.C.C. Historical Daily Station Observations (Temperature, Pressure, Precipitation, Sunshine Duration, etc.) for Germany, Version v21.3, 2021. (DWD), D.W., Ed. Offenbach, 2024.Available online: https://opendata.dwd.de/climate_environment/CDC/observations_germany/climate/daily/ (accessed on January 2024).

Fekete, B.M., Gibson, J.J., Aggarwal, P. and Vörösmarty, C.J., 2006. Application of isotope tracers in continental scale hydrological modeling. Journal of Hydrology, 330(3-4), pp.444-456.

Gat, J.R. and Gat, J.R., 1978. Isotope hydrology of inland sabkhas in the Bardawil area, Sinai. Limnology and Oceanography, 23(5), pp.841-850.

Gat, J.R., 1981. Properties of the isotopic species of water: the ‘‘isotope effect’’. Stable Isotope Hydrology, Deuterium and Oxygen-18 in the Water Cycle, IAEA Tech. Rep. Ser, (210), pp.7-19.

Gat, J.R., 1995. Stable isotopes of fresh and saline lakes. In Physics and chemistry of lakes (pp. 139-165). Berlin, Heidelberg: Springer Berlin Heidelberg.

Germer, S., Kaiser, K., Bens, O. and Hüttl, R.F., 2011. Water balance changes and responses of ecosystems and society in the Berlin-Brandenburg region–a review. DIE ERDE–Journal of the Geographical Society of Berlin, 142(1-2), pp.65-95.

Gerstengarbe, F.W., Badeck, F.W., Hattermann, F., Krysanova, V., Lahmer, W., Lasch, P., Stock, M., Suckow, F., Wechsung, F. and Werner, P.C., 2003. Studie zur klimatischenEntwicklung im Land Brandenburg bis 2055 und deren Auswirkungenauf den Wasserhaushalt, die Forst- und Landwirtschaft sowie dieAbleitung erster Perspektiven. Report No. 83, Potsdam Institute for Climate Impact Research (PIK).

Gerstengarbe, F.W., Werner, P.C., Österle, H. and Burghoff, O., 2013. Winter storm-and summer thunderstorm-related loss events with regard to climate change in Germany. Theoretical and applied climatology, 114, pp.715-724.

Gibson, J.J. and Reid, R., 2010. Stable isotope fingerprint of open-water evaporation losses and effective drainage area fluctuations in a subarctic shield watershed. Journal of Hydrology, 381(1-2), pp.142-150.

Gibson, J.J. and Reid, R., 2014. Water balance along a chain of tundra lakes: A 20-year isotopic perspective. Journal of Hydrology, 519, pp.2148-2164.

Gibson, J.J. and Reid, R., 2014. Water balance along a chain of tundra lakes: A 20-year isotopic perspective. Journal of Hydrology, 519, pp.2148-2164.

Hartwich, R., Eckelmann, W., Krug, D. and Thiele, S., 2007. Bodenübersichtskarte 1: 200 000 (BÜK 200). Status und Perspektiven. Mitt. Dtsch. Bodenkundl. Ges, 110(2), pp.449-450.

Herbst, M. and Kappen, L., 1999. The ratio of transpiration versus evaporation in a reed belt as influenced by weather conditions. Aquatic botany, 63(2), pp.113-125.

Hermanns, S. 2022. Creation of a hydrogeological conceptual model for the Lake Gross Glienicke and Sacrow, Berlin-Brandenburg. Master's thesis, Freie University Berlin.

Herrera, P.A., Marazuela, M.A. and Hofmann, T., 2022. Parameter estimation and uncertainty analysis in hydrological modeling. Wiley Interdisciplinary Reviews: Water, 9(1), p.e1569.

Jafari, T., Kiem, A.S., Javadi, S., Nakamura, T. and Nishida, K., 2021. Using insights from water isotopes to improve simulation of surface water-groundwater interactions. Science of The Total Environment, 798, p.149253.

Jänicke, B., Meier, F., Fenner, D., Fehrenbach, U., Holtmann, A., Scherer, D. (2017): Urban-rural differences in near-surface air temperature as resolved by the Central Europe Refined analysis (CER): sensitivity to planetary boundary layer schemes and urban canopy models. Int. J. Climatol. 37 (4), 2063-2079. DOI: 10.1002/joc.4835.

Kristensen, K.J., Jensen, S.E., 1975. A model for estimating actual evapotranspiration from potential evapotranspiration. Hydrology Research 1 June 1975; 6 (3): 170–188. doi: https://doi.org/10.2166/nh.1975.0012

Lahmer, W. and Pfützner, B., 2003. Orts-und zeitdiskrete Ermittlung der Sickerwassermenge im Land Brandenburg auf der Basis flächendeckender Wasserhaushaltsberechnungen. PIK.

Liu, Y. and Gupta, H.V., 2007. Uncertainty in hydrologic modeling: Toward an integrated data assimilation framework. Water resources research, 43(7).

Lüder, B., Kirchner, G., Lücke, A. and Zolitschka, B., 2006. Palaeoenvironmental reconstructions based on geochemical parameters from annually laminated sediments of Sacrower See (northeastern Germany) since the 17th century. Journal of Paleolimnology, 35, pp.897-912.

Mahmoodi, N., Kiesel, J., Wagner, P.D. and Fohrer, N., 2020. Integrating water use systems and soil and water conservation measures into a hydrological model of an Iranian Wadi system. Journal of Arid Land, 12(4), pp.545-560.

Mayr, C., Lücke, A., Stichler, W., Trimborn, P., Ercolano, B., Oliva, G., Ohlendorf, C., Soto, J., Fey, M., Haberzettl, T. and Janssen, S., 2007. Precipitation origin and evaporation of lakes in semi-arid Patagonia (Argentina) inferred from stable isotopes ($\delta^{18}O$, $\delta^{2}H$). Journal of Hydrology, 334(1-2), pp.53-63.

https://doi.org/10.5194/hess-2024-214
Preprint. Discussion started: 9 September 2024

Hydrology and Earth System Sciences
Discussions

Merrick, D., 2017. AlgoCompute Cloud-Computing Platform. Canberra, Australia: HydroAlgorithmics Pty Ltd.

Merz, C. and Pekdeger, A., 2011. Anthropogenic changes in the landscape hydrology of the Berlin-Brandenburg region. DIE ERDE–Journal of the Geographical Society of Berlin, 142(1-2), pp.21-39.

Mügler, I., Sachse, D., Werner, M., Xu, B., Wu, G., Yao, T. and Gleixner, G., 2008. Effect of lake evaporation on δD values of lacustrine n-alkanes: A comparison of Nam Co (Tibetan Plateau) and Holzmaar (Germany). Organic Geochemistry, 39(6), pp.711-729.

Müller Schmied, H., Eisner, S., Franz, D., Wattenbach, M., Portmann, F.T., Flörke, M. and Döll, P., 2014. Sensitivity of simulated global-scale freshwater fluxes and storages to input data, hydrological model structure, human water use and calibration. Hydrology and Earth System Sciences, 18(9), pp.3511-3538.

Myneni, R., Knyazikhin, Y. and Park, T., 2021. MODIS/Terra leaf area index/FPAR 8-day L4 global 500m SIN grid V061 [data set]. NASA EOSDIS Land Processes DAAC.

Ölmez, C., Tügel, F., & Hinkelmann, R., 2024. Sinking Water Level of Groß Glienicker See – A Data-Based Model for Estimating the Water Balance. Presented at Day of Hydrology conference, Berlin, Germany, 19-21 March 2024.

Partington, D., Knowling, M.J., Simmons, C.T., Cook, P.G., Xie, Y., Iwanaga, T. and Bouchez, C., 2020. Worth of hydraulic and water chemistry observation data in terms of the reliability of surface water-groundwater exchange flux predictions under varied flow conditions. Journal of Hydrology, 590, p.125441.

Pfannerstill, M., Guse, B. and Fohrer, N., 2014. Smart low flow signature metrics for an improved overall performance evaluation of hydrological models. Journal of Hydrology, 510, pp.447-458.

Renard, B., Kavetski, D., Kuczera, G., Thyer, M. and Franks, S.W., 2010. Understanding predictive uncertainty in hydrologic modeling: The challenge of identifying input and structural errors. Water Resources Research, 46(5).

Schaap, M.G., Leij, F.J. and Van Genuchten, M.T., 2001. Rosetta: A computer program for estimating soil hydraulic parameters with hierarchical pedotransfer functions. Journal of Hydrology, 251(3-4), pp.163-176.

https://doi.org/10.5194/hess-2024-214
Preprint. Discussion started: 9 September 2024

Schmidt, A., Frank, G., Stichler, W., Duester, L., Steinkop, T. & C. Stumpp (2020): Overview of tritium records from precipitation and surface waters in Germany. Hydrol. Process., 34, 1489-1493.

Singh, V.P., 2018. Hydrologic modeling: progress and future directions. Geoscience letters, 5(1), pp.1-18.

Skrzypek, G., Mydłowski, A., Dogramaci, S., Hedley, P., Gibson, J.J. and Grierson, P.F., 2015. Estimation of evaporative loss based on the stable isotope composition of water using Hydrocalculator. Journal of Hydrology, 523, pp.781-789.

Stumpp, C., Klaus, J. and Stichler, W., 2014. Analysis of long-term stable isotopic composition in German precipitation. Journal of Hydrology, 517, pp.351-361.

Tweed, S., Leblanc, M. and Cartwright, I., 2009. Groundwater–surface water interaction and the impact of a multi-year drought on lakes conditions in South-East Australia. Journal of Hydrology, 379(1-2), pp.41-53.

Vyse, S.A., Taie Semiromi, M., Lischeid, G. and Merz, C., 2020. Characterizing hydrological processes within kettle holes using stable water isotopes in the Uckermark of northern Brandenburg, Germany. Hydrological processes, 34(8), pp.1868-1887.

Welhan, J.A. and Fritz, P., 1977. Evaporation pan isotopic behavior as an index of isotopic evaporation conditions. Geochimica et Cosmochimica Acta, 41(5), pp.682-686.

Windhorst, D., Kraft, P., Timbe, E., Frede, H.G. and Breuer, L., 2014. Stable water isotope tracing through hydrological models for disentangling runoff generation processes at the hillslope scale. Hydrology and Earth System Sciences, 18(10), pp.4113-4127.

Wolter, K.D. and Ripl, W., 1999. Successful restoration of Lake Gross-Glienicker (Berlin, Brandenburg) with combined iron treatment and hypolimnetic aeration. In 8th International Conference on the Conservation and Managment of Lakes. Kopenhagen, Dänemark.

Wolter, K.D., 2010. Restoration of eutrophic lakes by phosphorus precipitation, with a case study on Lake Gross-Glienicker. Restoration of Lakes, Streams, Floodplains, And Bogs in Europe: Principles and Case Studies, pp.85-99.

Zhao, G., Li, Y., Zhou, L. and Gao, H., 2022. Evaporative water loss of 1.42 million global lakes. Nature Communications, 13(1), p.3686.